Controlling the Adsorption of Aromatic Compounds on Pt(111) with Oxygenate Substituents: From DFT to Simple Molecular Descriptors

Romain Reocreux, Minh Huynh, Carine Michel, Philippe Sautet

Controlling the Adsorption of Aromatic Compounds on Pt(111) with Oxygenate Substituents: From DFT to Simple Molecular Descriptors.

Romain Réocreux, Minh Huynh, Carine Michel,* and Philippe Sautet*

Université de Lyon, Université Claude Bernard Lyon 1, École Normale Supérieure de Lyon, Centre Nationale de Recherche Scientifique, 46 allée d'Italie, Lyon F-69007, France

E-mail: carine.michel@ens-lyon.fr; philippe.sautet@ens-lyon.fr

Abstract

Aromatic chemistry on metallic surfaces is involved in many processes within the contexts of biomass valorisation, pollutants degradation or corrosion protection. Albeit theoretically and experimentally challenging, knowing the structure and the stability of aromatic compounds on such surfaces is essential to understand their properties. To gain insights on this topic, we performed periodic *ab initio* calculations on Pt(111) to determine a set of simple molecular descriptors that predict both the stability and the structure of aromatic adsorbates substituted with *alkyl* and *alkoxy* (or *hydroxy*) groups. While the van der Waals (vdW) interaction is controlled by the molecular weight, and the deformation energy by both the nature and the relative position of the substituents to the surface, the chemical bonding can be correlated to the Hard and Soft Acids and Bases (HSAB) interaction energy. This work gives general insights on the interaction of aromatic compounds with the Pt(111) surface.

Graphical TOC Entry

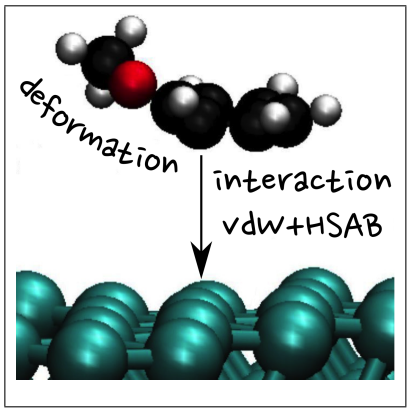

Keywords

aromatic, Pt(111), adsorption, DFT, HSAB, dispersion, deformation

The adsorption of substituted aromatics at metallic surfaces is of great interest in a wide range of domains, from corrosion protection[1–3] to the degradation of pollutants. Among them, oxygenates are of particular interest. Besides some examples of phenol synthesis from the heterogeneous oxidation of benzene,[4,5] most of the studies reported in the literature have focused on their decomposition. Phenolic compounds are indeed very toxic polluants[6] (*e.g.* dyes and endocrine disruptors) and, at the same time, commonly used as models to understand the decomposition and deoxygenation of lignin, a biomass polymer that might become a sustainable source of aromatics in the future.[7–10] Those transformations can be performed in reducing or oxidative media using a metallic surface, the catalytic activity of which is related to the adsorption energies of the intermediates as the Sabatier principle suggests. This has been developed quantitatively by the mean of volcano plots and Brønsted-Evans-Polanyi linear relationships.[11] Using such tools, one can rapidly predict the activity of a catalyst knowing how it interacts with the reactant or the intermediates. This is all the more important that today there is a need in rapid screening of catalysts to optimize industrial processes.

Theoretical chemistry and surface science are important methods to understand how those particular chemicals adsorb on metallic surfaces. Vibrational spectroscopies[12,13] and Scanning Tunneling Microscopy[14,15] provide structural features while Temperature Program Desorption (TPD)[16] and microcalorimetry experiments[17] allow us to quantify the affinity of the aromatic adsorbate to the metallic surface by the mean of heats of adsorption. On the theoretical side, Density Functional Theory (DFT) is now widely used to characterize adsorption geometries with their computed adsorption energies. The early studies by Morin *et al.*[18] determined the predominant structures of benzene on Pt(111) even though the GGA (generalized gradient approximation) calculations markedly underestimate the experimental adsorption energies. Many other aromatics on different metal surfaces have been reported with such method.[19–22] Since then, more advanced DFT methods have been developed to account accurately for dispersion interactions.[23,24] Some of those functionals provide a much better estimation of the aromatic adsorption energies.[25,26] Other DFT methods, such as the Random Phase Approximation, are known to be among the most accurate calculations for adsorption on metals but remain computationally extremely expensive.[27]

Despite that remarkable evolution toward experimental and theoretical accuracy over the years, all those techniques are very time-demanding and they rarely provide chemical trends that can easily be exploited by both experimentalists and theoreticians.[21,28,29] Notwithstanding, there are many examples of simple aromatic descriptors widely used to account for various chemical properties. Those can be geometry descriptors (Holleman's product rule) or electronic descriptors (Hammett parameters or frontier orbital and Pearson's descriptors). They do not aim at describing the properties very accurately but they definitely are very useful and popular rules of thumb.

In this work, we investigate the adsorption of a range of alkyl and alkoxy substituted aromatics (see Figure 1) on a Pt(111) surface with periodic PBE-dDsC calculations (see SI for a description of methods). Beyond the DFT numbers, we propose simple trends that enable the understanding and the prediction of the influence of substituents on aromatic adsorption. In the set, there are different kinds of aromatic compounds, mostly biomass-derivated oxygenates, the substituents of which are mainly linked to the aromatic ring via an oxygen or a carbon atom. Therefore we will distinguish between O-substituents and C-substituents. To that set, we added toluene and benzene: the former to isolate the effect of C-substituents, and the latter to compare with the simplest aromatic chemical.

The very studied benzene on Pt(111), albeit not substituted, is a clear starting point. It predominantly adsorbs at bri30 and hcp0 sites (see Figure 2), the later being the most stable.[18,25,26] In that nomenclature the position of the centre of the flat-lying aromatic adsorbate is first given (hcp, bri, fcc or top) followed by the ide-

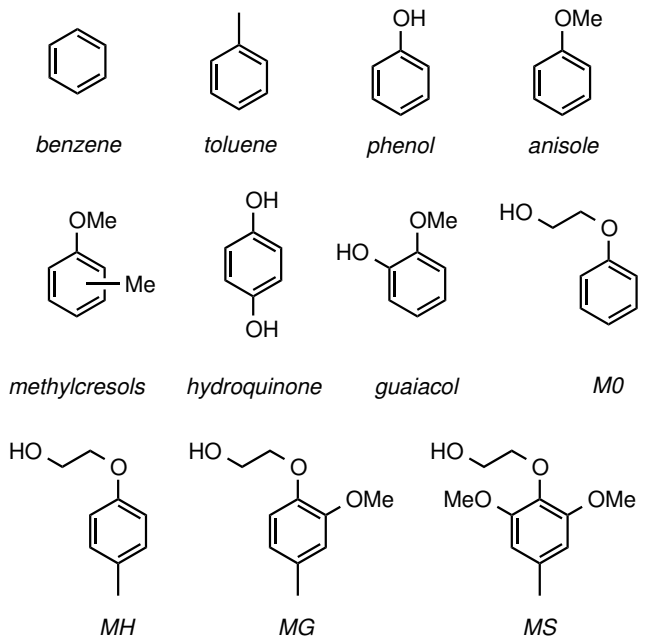

Figure 1: Set of aromatic compounds studied in this work. It consists of common mono and polysubstituted aromatic oxygenates. M0 is a simple β-O-4 linkage model of lignin. MH, MG and MS are derivates of M0 meant to account for the very specific environnement of the hydroxyphenyl (H), guaiacyl (G) and syringyl (S) moieties of lignin. Benzene and toluene are added as non oxygenated aromatic derivates.

alized value of the angle between the aromatic C–C direction and the Pt(111) close-packed orientation (see Figure 2). Upon adsorption the ring gets slightly deformed and the hydrogens are bent away from the surface. To account for the latter effect, we introduce the out-of-plane deformation angle Θ (see Scheme 1 for the graphical definition). At the hcp0 site, the aromatic carbons are strictly equivalent: they are bound – in pairs – to the surface in a way that is very similar to π-bonded ethylene (with $\Theta = 20°$). They will therefore be labelled π. At the bri30 site, we can find two pairs of π carbons as well (with $\Theta = 18°$) but also two other carbons – in *para* position to each other – that show a bigger deformation angle ($\Theta = 34°$) and a much more tetrahedral geometry as σ-bonded carbonated species would. They will therefore be labelled σ. What about the substituted aromatics? Where shall we put the substituent(s)

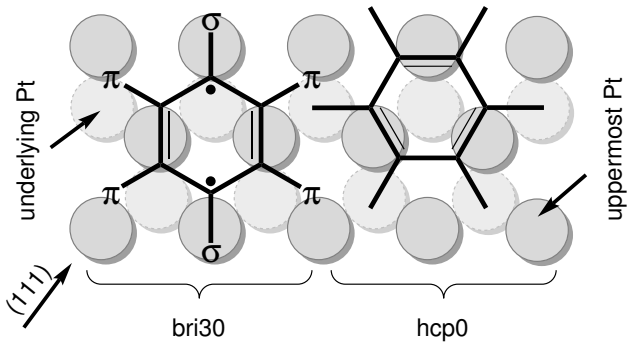

Figure 2: The two most stable adsorption sites of benzene: hcp0 on the right (all the substitution positions being equivalent) and bri30 on the left (with the two substitution positions: σ and π).

to get the most stable structure? On π or σ carbons ? Do(es) the substituent(s) influence the position of the aromatic ring on the surface? To answer these questions, we limited the DFT inspection to those most stable bri30 and hcp0 sites since the other adsorption modes are at least about 0.3 eV less stable.

Table 1: Energy and geometry features of anisole and toluene structures on Pt(111).

Adsorption site	bri30		hcp0
Substituent position	π	σ	π
Anisole			
Deformation angle Θ	24°	44°	24°
Relative stability (eV)	0	0.11	0.29
Toluene			
Deformation angle Θ	26°	40°	27°
Relative stability (eV)	0	0.002	0.25
Benzene			
Deformation angle Θ	18°	34°	20°
Relative stability (eV)	0		0.26

Let's start with two simple monosubstituted aromatic compounds: an O-substituted one, namely anisole, and a C-substituted one, namely toluene. We have to consider two geometries at the bri30 site, the substituent being either on a π or an σ carbon, and one at the hcp0 site. Anisole and toluene show the same preference for the bri30 adsorption site over

hcp0 with an energy difference of about 0.3 eV (see Table 1). This energy difference does not seem to be related to any increased deformation (similar deformation angle as in the most stable bri30 geometry) but rather a commun feature to many aromatic compounds. The same energy difference was indeed computed for benzene by Morin *et al.*[18] and the bri30 structure was also reported for anisole[30] and other aromatic compounds such as phenol,[22] guaiacol[31,32] and halogenobenzenes.[28] Regarding substitution at the bri30 adsorption site, toluene does not really show any preference for a π or σ position even if the deformation angle is almost doubled between the first and the second geometry. Unlike toluene, anisole is much more sensitive to the substitution position: with a very similar variation of the deformation angle, the σ position is less stable than the π position by 0.11 eV. From those observations, one can go further and search for simple molecular descriptors giving a picture of the adsorption at the most stabilizing bri30 site. Since deformation seems to play a role, we will decompose the adsorption energy into three terms as follows:

$$E_{ads} = E_{def} + E_{\phi} + E_{\chi} \tag{1}$$

where E_{def}, E_{ϕ} and E_{χ} stand for the deformation energy, the physical (dispersion interaction) and the chemical part of the total interaction energy respectively (see the associated Hess cycle in Scheme 1).

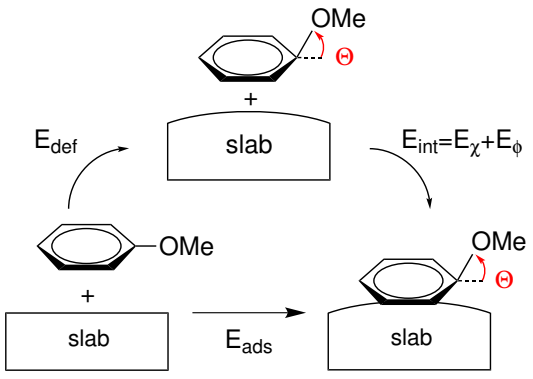

Scheme 1: Hess cycle for anisole adsorption involving the deformations of the molecule (quantified by the out-of-plane deformation angle Θ) and the slab.

What molecular descriptors do those energetic contributions depend on?

Dispersion interaction. The dispersion interaction is known to be proportional to the polarizability of the molecules. According to the Clausius-Mossotti relation,[33] the polarizability is proportional to the molecular weight. From semi-classical physics (see details in SI), we can estimate the dispersion interaction energy of a compound (molecular weight M at a height of Z) with a metallic surface as follows:

$$E_{disp} \simeq -k\frac{M}{Z^3} \tag{2}$$

with $k \simeq 0.3\,\text{eV Å}^3\,\text{mol g}^{-1}$ for typical organic compounds. For the aromatic compounds we considered (molecular weight M), we have therefore the contributions of both the aromatic ring (molecular weight M_0, height $Z_0 \simeq 3$ Å) that lies closer to the surface than the substituent(s) (molecular weight M', height $Z' \simeq 3.5$ Å). Adding the two contributions and considering that $M' = M - M_0$, we get:

$$\begin{aligned} E_{disp} &= -k\left(\frac{M_0}{Z_0^3} + \frac{M'}{Z'^3}\right) \\ &= -\frac{k}{Z'^3} \times M - k\left(\frac{M_0}{Z_0^3} - \frac{M_0}{Z'^3}\right) \end{aligned} \tag{3}$$

We obtain from equation (3) the relation $E_{disp} = aM + b$ with $a = -7 \cdot 10^{-3}$ eV mol/g and $b = -0.3$ eV. That agrees very well with the DFT PBE-dDsC results that show a very similar linear relationship (E_{disp} in eV and M in g/mol, Figure 3a) with a very small mean absolute deviation (MAD):

$$E_{disp} = -6.7 \cdot 10^{-3} M - 0.25 \quad \text{MAD} = 0.04\ \text{eV}$$

Although dispersion interactions are important to estimate properly the adsorption energies of flat-flying conjugated molecules,[26] it does interestingly not depend on the π/σ distinction and probably explains why GGA calculations are still relevant for energy differences but not for absolute energies.

Deformation energies. The deformation energy should depend on the total number of substituents n since there are more functional

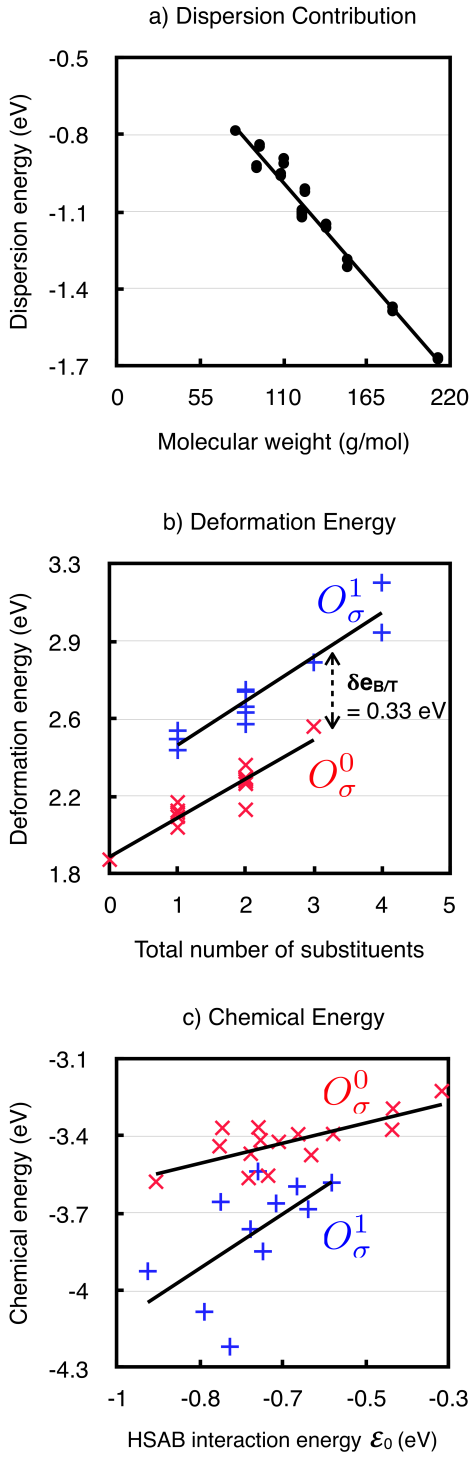

Figure 3: Energy decomposition over the set of molecules defined in Figure 1: (a) physical interaction (b) deformation energy (c) chemical interaction energy. In the last two diagrams: $\times$ adsorption mode with all hydroxy/alkoxy groups at a π position (sub-set O^0_σ); + adsorption mode with one hydroxy/alkoxy group at a σ position (sub-set O^1_σ).

groups to be bent from the ring plane. That is why we plotted the deformation energy as a function of the total number of substituents (Figure 3b). In order to account for the sensitivity of O-substituents to the π/σ positions, the whole set was divided into two sub-sets: the first sub-set consisting of adsorbates without any O-substituents at the σ positions (no constraints on the C-substituents though) and the second sub-set consisting of adsorbates with one, and one only, O-substituent at a σ position. For the former – referred to as O^0_σ – we can see that the deformation energy (in eV) increases linearly with the total number of substituents n:

$$E_{def}(O^0_\sigma) = 0.19n + 1.88 \qquad \text{MAD} = 0.04 \text{ eV}$$

for the later – referred to as O^1_σ – the same behaviour is observed :

$$E_{def}(O^1_\sigma) = 0.21n + 2.21 \qquad \text{MAD} = 0.06 \text{ eV}$$

It means there is the same deformation energy cost of *ca.* 0.2 eV per substituent and it is additive. That was already pointed out by Peköz *et al.*[28] who studied different polyhalogenobenzenes on Pt(111): the deformation being about 0.3 eV per substituent. However they did not distinguish between π and σ positions, the influence of which is a $\delta e_{\pi/\sigma} = 0.33$ eV off-set for O-substituents.

Chemical interaction energies. To rationalise chemical interactions, there are several approaches. One of them is Pearson's Hard and Soft Acids and Bases (HSAB) theory.[34,35] This theory describes the interaction between two species A and B in terms of their chemical hardness η_A and η_B and their electron chemical potential μ_A and μ_B that can be seen as the opposite of their electronegativity. The interaction induces an electronic flow (from high to lower chemical potentials) associated with the following HSAB stabilisation energy $\mathcal{E}$:

$$\mathcal{E} = -\frac{1}{4}\frac{(\mu_A - \mu_B)^2}{\eta_A + \eta_B} < 0 \qquad (4)$$

Within the finite difference approximation and the frontier orbital approximation, Pearson

proposed to estimate the chemical hardness η_i and the electron chemical potential μ_i as follows:

$$\mu_i \simeq \begin{cases} \frac{1}{2}\left(E_{LUMO} + E_{HOMO}\right) & \text{for molecules} \\ \varepsilon_F & \text{for solids} \end{cases} \quad (5)$$

$$\eta_i \simeq \begin{cases} \frac{1}{2}\left(E_{LUMO} - E_{HOMO}\right) & \text{for molecules} \\ \frac{1}{2}BG & \text{for solids} \end{cases} \quad (6)$$

where E_{LUMO}, E_{HOMO}, ε_F and BG stand for the energies of the lowest unoccupied molecular orbital energy, the highest occupied molecular orbital energy, the Fermi level and the band gap respectively. For a metal, the band gap is zero. Therefore the HSAB interaction energy simply writes:

$$\mathcal{E} = -\frac{(\mu - \varepsilon_F)^2}{4\eta} < 0 \quad (7)$$

where μ and η stand for the adsorbate parameters. Literature shows examples where this interaction energy $\mathcal{E}$ is used quantitatively.[36] Such a quantitative treatment is however accurate only if the geometries of the two interacting parts do not change significantly upon interaction. Otherwise HSAB theory gets much more complex to account for the external potential variations but still allows – in its simpler form – to understand chemical interaction at metal surfaces.[37] For the purpose of simplicity (and predictability) we will correlate the actual DFT interaction energy with its HSAB counterpart evaluated from **the totally relaxed gas phase structures** (μ_0 and η_0) referred to as $\mathcal{E}_0$:

$$\mathcal{E}_0 = -\frac{(\mu_0 - \varepsilon_F)^2}{4\eta_0} < 0 \quad (8)$$

where both $(\mu_0 - \varepsilon_F)$ and η_0 are positive quantities. Plotting the DFT chemical interaction energies as a function of the HSAB interaction energies (Figure 3c), we get for the first sub-set O^0_σ:

$$E_\chi(O^0_\sigma) = 0.45 \cdot \mathcal{E}_0 - 3.14 \qquad \text{MAD} = 0.05 \text{ eV}$$

and for the second sub-set O^1_σ, which consists of more deformed adsorbates:

$$E_\chi(O^1_\sigma) = 1.20 \cdot \mathcal{E}_0 - 2.92 \qquad \text{MAD} = 0.13 \text{ eV}$$

Because of the approximations we did, we expected the DFT chemical interaction energies E_χ to be different from the HSAB idealized interaction energies $\mathcal{E}_0$. Despite of that, we interestingly get a fair correlation with reasonable MAD and a positive slope (the bigger $\mathcal{E}_0$, the bigger E_χ) that is still of the order of 1. As for the intercept, it corresponds to the interaction energy between an adsorbate and a surface of identical electronegativities (or electron chemical potentials) $\mu_0 = \varepsilon_F$. In other words, the intercept is the covalent contribution to the overall chemical interaction and in the two subsets they are quite comparable (about 3 eV, hence 0.5 eV per aromatic carbon). Moreover, the chemical interaction in the more deformed O^1_σ sub-set is stronger than the less deformed O^0_σ sub-set. It can be interpreted in terms of chemical hardness. The Principle of Maximum Hardness[38] suggests that the gas phase structures maximize the chemical hardness: thus the molecules should get softer upon deformation. Since the metallic surface is extremely soft ($\eta_{Pt} = 0$), the deformation process indeed increases the intensity of the soft-soft interactions. Nonetheless, we showed that the deformation had its own energetic cost. Altogether the chemical part of the interaction energy favors the presence of an O-substituent at the σ position, and therefore competes with the effect of the deformation energy as discussed in the next section.

Prediction of adsorption energies and structures. By summing the fitted linear expressions obtained in the previous parts, one can give an estimation of the adsorption energies E_{ads} of the two sub-sets O^0_σ and O^1_σ :

$$E_{ads}(O^0_\sigma) = \alpha M + 0.45\mathcal{E}_0 + 0.19n - 1.51 \quad (9)$$

$$E_{ads}(O^1_\sigma) = \alpha M + 1.20\mathcal{E}_0 + 0.21n - 0.95 \quad (10)$$

with $\alpha = -6.7 \cdot 10^{-3}$ eV mol/g. Taking into account the molecular weight M, the total number of substituents n and the electronic effects through $\mathcal{E}_0$, our approach remarkably well ap-

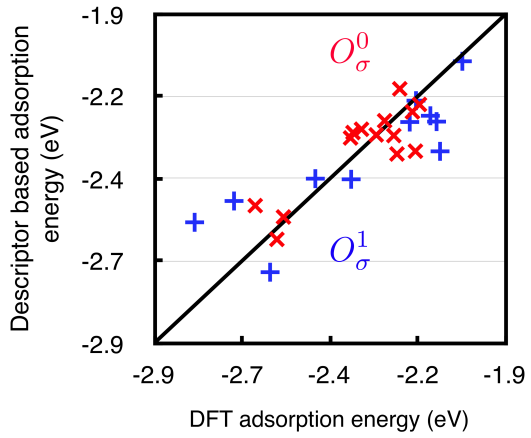

Figure 4: Descriptor-based adsorption energies as a function of the actual DFT computed adsorption energies. The full line corresponds to the identity.

proximates the actual adsorption energies computed with DFT (see the parity plot given in Figure 4). The overall mean absolute deviation is only 0.08 eV with a maximum absolute deviation of 0.25 eV, so our approach appears quite reliable. Thus, those relations are a fast screening tool for the adsorption of substituted aromatic oxygenates, predicting the energy and the structure, in line with the widely used scaling relations[31,39–43] More interestingly, our model also seems to depict – at least partly – the balance between the deformation energy (which tends to favor adsorption configuration without O substituent in the σ position) and the chemical interaction energy (which tends to favor adsorption modes with a O substituent at the σ position). The energy difference $\Delta_\sigma^{0/1}$ writes:

$$\begin{aligned}\Delta_\sigma^{0/1} &= E_{ads}(O^1_\sigma) - E_{ads}(O^0_\sigma) \\ &= 0.75\mathcal{E}_0 + 0.02n + 0.56\end{aligned} \quad (11)$$

The HSAB parameter $\mathcal{E}_0$ being negative, two regimes are possible. At small $\mathcal{E}_0$, the most favorable adsorption mode is the O^0_σ, with no O susbstituent at the σ position when possible. For large enough absolute values of $\mathcal{E}_0$, one should in principle see an inversion of this trend. This is indeed the case for MG that has the largest HSAB idealized interaction energy ($\mathcal{E}_0 = -0.94$ eV): the O^1_σ geometry is slightly more stable than the O^0_σ geometry with an energy difference of 0.01 eV (see SI for details).

Our correlations do not only allow to predict the adsorption energies and geometries from very simple molecular descriptors but they also help to understand the nature of the bond between aromatic oxygenates and Pt(111), a very typical surface for heterogeneous catalysis applications. It opens new strategies to rationalize chemical reactivities or the design of metallic catalysts since we showed that besides the Fermi level of the metal (or the related *d*-band centre), other parameters control adsorption such as the electronegativity (or electron chemical potential), the chemical hardness, the molecular weight and the adsorption geometry.

Acknowledgements

The authors are grateful to the Centre Blaise Pascal (CBP), the Pôle Scientifique de Modélisation Numérique (PSMN) – both at the École Normale Supérieure de Lyon – and the GENCI (CINES), project x2015080609 that provided assistance and calculation resources. They also thank the LIA FUNCAT collaboration for fundings.

Supporting Information Available: Computational details, pictures and full energy analysis of all the adsorbates mentioned, and derivation of equation (2). This material is available free of charge via the Internet at `http://pubs.acs.org/`.

References

(1) Gattinoni, C.; Michaelides, A. Understanding corrosion inhibition with van der Waals DFT methods: the case of benzotriazole. *Faraday Discuss.* **2015**, *180*, 439–458.

(2) Özcan, M.; Toffoli, D.; Üstünel, H.; Dehri, . Insights into surfaceadsorbate interactions in corrosion inhibition processes at the molecular level. *Corros. Sci.* **2014**, *80*, 482–486.

(3) Obot, I.; Macdonald, D.; Gasem, Z. Density functional theory (DFT) as a powerful tool for designing new organic corrosion inhibitors. Part 1: An overview. *Corros. Sci.* **2015**, *99*, 1–30.

(4) Orita, H.; Itoh, N. Simulation of phenol formation from benzene with a Pd membrane reactor: Ab initio periodic density functional study. *Appl. Catal. A Gen.* **2004**, *258*, 17–23.

(5) Niwa, S.-i. A One-Step Conversion of Benzene to Phenol with a Palladium Membrane. *Science* **2002**, *295*, 105–107.

(6) Nousir, S.; Keav, S.; Barbier, J.; Bensitel, M.; Brahmi, R.; Duprez, D. Deactivation phenomena during catalytic wet air oxidation (CWAO) of phenol over platinum catalysts supported on ceria and ceriazirconia mixed oxides. *Appl. Catal. B Environ.* **2008**, *84*, 723–731.

(7) Zakzeski, J.; Bruijnincx, P. C. A.; Jongerius, A. L.; Weckhuysen, B. M. The Catalytic Valorization of Lignin for the Production of Renewable Chemicals. *Chem. Rev.* **2010**, *110*, 3552–3599.

(8) Nimmanwudipong, T.; Runnebaum, R. C.; Block, D. E.; Gates, B. C. Catalytic Conversion of Guaiacol Catalyzed by Platinum Supported on Alumina: Reaction Network Including Hydrodeoxygenation Reactions. *Energy & Fuels* **2011**, *25*, 3417–3427.

(9) Hensley, A. J.; Wang, Y.; McEwen, J.-S. Adsorption of guaiacol on Fe (110) and Pd (111) from first principles. *Surf. Sci.* **2016**, *648*, 227–235.

(10) Gao, F.; Webb, J. D.; Hartwig, J. F. Chemo- and Regioselective Hydrogenolysis of Diaryl Ether CO Bonds by a Robust Heterogeneous Ni/C Catalyst: Applications to the Cleavage of Complex Lignin-Related Fragments. *Angew. Chemie Int. Ed.* **2016**, *55*, 1474–1478.

(11) Nørskov, J. K.; Bligaard, T.; Rossmeisl, J.; Christensen, C. H. Towards the computational design of solid catalysts. *Nat. Chem.* **2009**, *1*, 37–46.

(12) Lehwald, S.; Ibach, H.; Demuth, J. Vibration spectroscopy of benzene adsorbed on Pt(111) and Ni(111). *Surf. Sci.* **1978**, *78*, 577–590.

(13) Tan, Y.; Khatua, S.; Jenkins, S.; Yu, J.-Q.; Spencer, J.; King, D. Catalyst-induced changes in a substituted aromatic: A combined approach via experiment and theory. *Surf. Sci.* **2005**, *589*, 173–183.

(14) Weiss, P. S.; Eigler, D. M. Site Dependence of the Apparent Shape of a Molecule in Scanning Tunneling Microscope Images: Benzene on Pt(111). *Phys. Rev. Lett.* **1993**, *71*, 3139–3142.

(15) Sautet, P.; Bocquet, M.-L. A theoretical analysis of the site dependence of the shape of a molecule in STM images. *Surf. Sci. Lett.* **1994**, *304*, 445–450.

(16) Ihm, H.; White, J. M. Stepwise dissociation of thermally activated phenol on Pt(111). *J. Phys. Chem. B* **2000**, *104*, 6202–6211.

(17) Ihm, H.; Ajo, H. M.; Gottfried, J. M.; Bera, P.; Campbell, C. T. Calorimetric Measurement of the Heat of Adsorption of Benzene on Pt(111) . *J. Phys. Chem. B* **2004**, *108*, 14627–14633.

(18) Morin, C.; Simon, D.; Sautet, P. Chemisorption of Benzene on Pt(111), Pd(111), and Rh(111) Metal Surfaces : A Structural and Vibrational Comparison from First Principles. *J. Phys. Chem. B* **2004**, *108*, 5653–5665.

(19) Ghiringhelli, L. M.; Caputo, R.; Site, L. D. Phenol near Ni(111), Ni(110), and Ni(221) surfaces in a vertical ring geometry: A density functional study of the oxygen-surface bonding and O-H cleavage. *Phys. Rev. B* **2007**, *75*, 113403.

(20) Delle Site, L.; Alavi, A.; Abrams, C. F. Adsorption energies and geometries of phenol on the (111) surface of nickel: An ab initio study. *Phys. Rev. B* **2003**, *67*, 193406.

(21) Bonalumi, N.; Vargas, A.; Ferri, D.; Baiker, A. Theoretical and Spectroscopic Study of the Effect of Ring Substitution on the Adsorption of Anisole on Platinum. *J. Phys. Chem. B* **2006**, *110*, 9956–9965.

(22) Honkela, M. L.; Björk, J.; Persson, M. Computational study of the adsorption and dissociation of phenol on Pt and Rh surfaces. *Phys. Chem. Chem. Phys.* **2012**, *14*, 5849–5854.

(23) Steinmann, S. N.; Corminboeuf, C. Comprehensive benchmarking of a density-dependent dispersion correction. *J. Chem. Theory Comput.* **2011**, *7*, 3567–3577.

(24) Klimeš, J.; Michaelides, A. Perspective: Advances and challenges in treating van der Waals dispersion forces in density functional theory. *J. Chem. Phys.* **2012**, *137*, 120901–120913.

(25) Yildirim, H.; Greber, T.; Kara, A. Trends in Adsorption Characteristics of Benzene on Transition Metal Surfaces: Role of Surface Chemistry and van der Waals Interactions. *J. Phys. Chem. C* **2013**, *117*, 20572–20583.

(26) Gautier, S.; Steinmann, S. N.; Michel, C.; Fleurat-Lessard, P.; Sautet, P. Molecular adsorption at Pt(111). How accurate are DFT functionals? *Phys. Chem. Chem. Phys.* **2015**, *17*, 28921–28930.

(27) Schimka, L.; Harl, J.; Stroppa, A.; Grüneis, A.; Marsman, M.; Mittendorfer, F.; Kresse, G. Accurate surface and adsorption energies from many-body perturbation theory. *Nat. Mater.* **2010**, *9*, 741–744.

(28) Peköz, R.; Johnston, K.; Donadio, D. Tuning the Adsorption of Aromatic Molecules on Platinum via Halogenation. *J. Phys. Chem. C* **2014**, *118*, 6235–6241.

(29) Hensley, A. J.; Wang, Y.; McEwen, J.-S. Adsorption of phenol on Fe (110) and Pd (111) from first principles. *Surf. Sci.* **2014**, *630*, 244–253.

(30) Bonalumi, N.; Vargas, A.; Ferri, D.; Bürgi, T.; Mallat, T.; Baiker, A. Competition at Chiral Metal Surfaces: Fundamental Aspects of the Inversion of Enantioselectivity in Hydrogenations on Platinum. *J. Am. Chem. Soc.* **2005**, *127*, 8467–8477.

(31) Lee, K.; Gu, G. H.; Mullen, C. a.; Boateng, A. a.; Vlachos, D. G. Guaiacol Hydrodeoxygenation Mechanism on Pt(111): Insights from Density Functional Theory and Linear Free Energy Relations. *ChemSusChem* **2015**, *8*, 315–322.

(32) Lu, J.; Behtash, S.; Mamun, O.; Heyden, A. Theoretical Investigation of the Reaction Mechanism of the Guaiacol Hydrogenation over a Pt(111) Catalyst. *ACS Catal.* **2015**, *5*, 2423–2435.

(33) Atkins, P.; Paula, J. D. *Chemistry (Easton).*; 2010.

(34) Parr, R. G.; Pearson, R. G. Absolute hardness: companion parameter to absolute electronegativity. *J. Am. Chem. Soc.* **1983**, *105*, 7512–7516.

(35) Pearson, R. G. Hard and soft acids and bases, HSAB, part 1: Fundamental principles. *J. Chem. Educ.* **1968**, *45*, 581–587.

(36) Romero, M. d. L.; Méndez, F. The Local HSAB Principle and Bond Dissociation Energy of p -Substituted Phenol. *J. Phys. Chem. A* **2003**, *107*, 5874–5875.

(37) Kokalj, A. On the HSAB based estimate of charge transfer between adsorbates and metal surfaces. *Chem. Phys.* **2012**, *393*, 1–12.

(38) Geerlings, P.; De Proft, F.; Langenaeker, W. Conceptual Density Functional

Theory. *Chem. Rev.* **2003**, *103*, 1793–1874.

(39) Ferrin, P.; Simonetti, D.; Kandoi, S.; Kunkes, E.; Dumesic, J. A.; Nørskov, J. K.; Mavrikakis, M. Modeling ethanol decomposition on transition metals: a combined application of scaling and Brønsted-Evans-Polanyi relations. *J. Am. Chem. Soc.* **2009**, *131*, 5809–5815.

(40) Liu, B.; Greeley, J. Decomposition pathways of glycerol via C-H, O-H, and C-C bond scission on Pt(111): A density functional theory study. *J. Phys. Chem. C* **2011**, *115*, 19702–19709.

(41) Sutton, J. E.; Vlachos, D. G. A Theoretical and Computational Analysis of Linear Free Energy Relations for the Estimation of Activation Energies. *ACS Catal.* **2012**, *2*, 1624–1634.

(42) Calle-Vallejo, F.; Tymoczko, J.; Colic, V.; Vu, Q. H.; Pohl, M. D.; Morgenstern, K.; Loffreda, D.; Sautet, P.; Schuhmann, W.; Bandarenka, A. S. Finding optimal surface sites on heterogeneous catalysts by counting nearest neighbors. *Science* **2015**, *350*, 185–189.

(43) Calle-Vallejo, F.; Loffreda, D.; Koper, M. T. M.; Sautet, P. Introducing structural sensitivity into adsorptionenergy scaling relations by means of coordination numbers. *Nat. Chem.* **2015**, *7*, 403–410.